

## Laboratory Test of the Isotropy of Light Propagation at the $10^{-17}$ Level

Ch. Eisele, A. Yu. Nevsky, and S. Schiller

*Institut für Experimentalphysik, Heinrich-Heine-Universität Düsseldorf, 40225 Düsseldorf, Germany*  
(Received 13 June 2008; revised manuscript received 7 August 2009; published 25 August 2009)

We report on the results of a strongly improved test of local Lorentz invariance, consisting of a search for an anisotropy of the resonance frequencies of electromagnetic cavities. The apparatus comprises two orthogonal standing-wave optical cavities interrogated by a laser, which were rotated approximately 175 000 times over the duration of 13 months. The measurements are interpreted as a search for an anisotropy of the speed of light, within the Robertson-Mansouri-Sexl (RMS) and the standard model extension (SME) photon sector test theories. We find no evidence for an isotropy violation at a  $1\sigma$  uncertainty level of 0.6 parts in  $10^{17}$  (RMS) and 2 parts in  $10^{17}$  for seven of eight coefficients of the SME.

DOI: 10.1103/PhysRevLett.103.090401

PACS numbers: 03.30.+p, 11.30.Cp

The principle of local Lorentz invariance (LLI) states that any physical process in an inertial laboratory evolves independently of the latter's state of motion and of its orientation. LLI is a postulate of the current theories of the fundamental interactions, general relativity and the standard model. However, theoretical work towards a unified theory of all forces suggests that LLI may only be an approximate principle. This motivates experimental tests of LLI with increased sensitivity. Recent experiments on different microscopic and macroscopic systems, as well as astronomical tests have not found any violation [1–16].

One aspect of local Lorentz invariance, the isotropy of space, can be tested with Michelson-Morley-type experiments [17]. According to the conventional interpretation, they search for a possible dependence of the speed of light on the propagation direction. Within the Robertson-Mansouri-Sexl (RMS) test theory of special relativity [18,19], a classical test theory, this experiment type provides one of three experiments required to determine the form of the Lorentz transformations, the others being a measurement of time dilation [15] and a test of the independence of the speed of light from the speed of the laboratory [16]. Within a modern field theoretical description of LLI violation, the standard model extension (SME) [20], it is shown that Michelson-Morley-type experiments are sensitive to at least eight independent coefficients that determine the contribution of certain terms in the LLI violating Lagrangian [12,21]. Confining the analysis of a Michelson-Morley-type experiment to the photonic sector of that Lagrangian, also leads to the interpretation of a variable speed of light.

In this Letter we report on an isotropy test experiment with significantly improved sensitivity compared to previous ones [2–6,10]. Its sensitivity to isotropy violation signatures (the beat frequency modulation amplitudes B, C, see below) is at the level of less than 1 part in  $10^{15}$  per rotation, and averaging over a large number of rotations, allowed us reaching the level of a few parts in  $10^{17}$ .

Our apparatus is shown in Fig. 1 and a preliminary description of the apparatus has been given in Ref. [22]. It

comprises a pair of orthogonally oriented optical standing-wave cavities interrogated by laser waves [Fig. 1(a)]. The laser waves' frequencies are kept equal to the cavity frequencies  $\nu_1$ ,  $\nu_2$ . The difference  $\nu_1 - \nu_2$  ("beat frequency") is the quantity of interest—a test of isotropy consists in searching for a change of the beat frequency with changing orientation in space. The main design aim was a high dimensional stability of the cavities and a precise readout of the cavities' frequencies  $\nu_1$ ,  $\nu_2$  by the laser. Salient features of the apparatus, shown in Fig. 1(b), are the following: an air cushion rotation table with low axis wobble and low vibration level; active stabilization of the normal of the optics breadboard during rotation; an active vibration isolation system that reduces the acceleration level present on the optical plate; optical cavities with low thermal noise; low thermal sensitivity; precision frequency locking of the laser wave to the cavities. The rotation table consists of a 1.3 ton octagonal granite base on which a cross-shaped frame moves on a thin air cushion. The axis of the frame is held and stabilized in the horizontal plane by a radial air bearing, which also provides a rotary feed-through for power supply and signals. The rotational motion is produced by a set of piezoelectric translators. The rotational axis shows a very small wobble (few  $\mu\text{rad}$ ) with respect to the base. However, the tilt of the laboratory floor and therefore the average rotation axis direction is not constant in time. To compensate for this effect, the tilt of the base plate of the rotation table is stabilized using an air spring system, and the optics breadboard carrying the cavities is additionally placed on a base that regulates the residual tilt and provides active vibration isolation.

In our implementation, the two cavities are contained in a single block of glass with ultralow thermal expansion coefficient (ULE). The cavities (lengths  $L_i = 8.4$  cm) have mode linewidths of approximately 10 kHz. A Nd:YAG laser ( $\nu_0 = 282$  THz) is used for interrogation. A single laser performs the interrogation of the two cavities by splitting its wave in two individually frequency-tunable waves by means of acousto-optical frequency shifters AOM1, AOM2 [see Fig. 1(a)]. The waves' frequencies

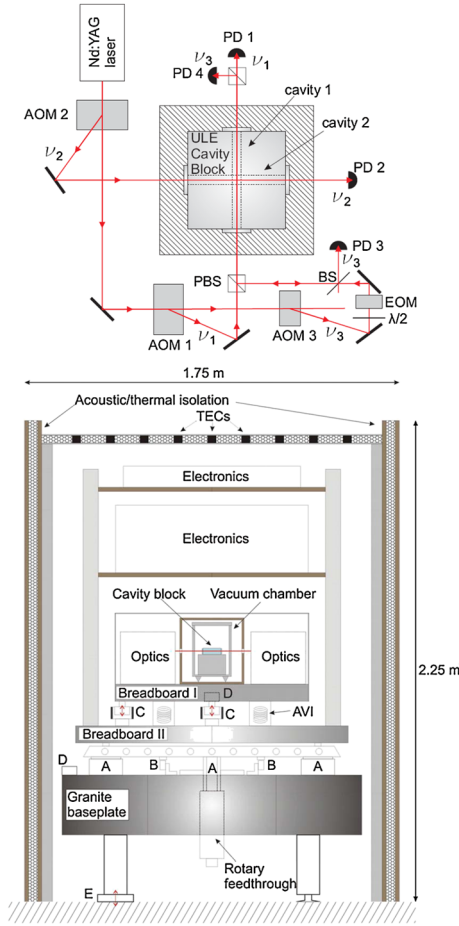


FIG. 1 (color online). (a) schematic of the optical setup. The ULE cavity block is temperature stabilized inside a vacuum chamber (textured area). The wave  $\nu_3$  is used for prestabilizing the frequency of the laser to a  $TEM_{01}$  mode of one cavity. PD1, PD2, PD3 are detectors used to generate error signals for controlling the frequencies of AOM1, AOM2 and the laser itself, respectively. PD4 monitors the transmitted power of wave  $\nu_3$ . PD, photodetector; AOM, acousto-optic frequency shifter and modulator; EOM, electrooptic phase modulator; PBS, polarization beam splitter (BS). (b) Side cutaway view of the whole apparatus. A, air cushion or bearing; B, rotary motor; C, voice coil actuators; D, two-axis tilt sensor; E, air spring system; TEC, thermoelectric cooler elements for temperature regulation.

are then stabilized to two  $TEM_{00}$  modes (frequencies  $\nu_1$ ,  $\nu_2$ ) of the respective cavities [22].

The beat frequency was measured with a counter with an integration time of 1 s. Its value and other parameters such as the rotation angle, tilts, laser powers transmitted through the cavities, tilt actuator voltages, and temperature inside the housing were acquired at a rate of 1/s.

The apparatus was characterized by determining the noise level of the beat frequency (minimum detectable change in  $\nu_1 - \nu_2$ ) and systematic effects.

The beat frequency drifted in time at a varying rate  $a \nu_0$ , not exceeding 1.5 Hz/s, and this was taken into account in the data analysis (see below). Under rotation, the beat instability [root Allan variance of the short-term beat fre-

quency fluctuations  $N_i(t) \nu_0$ ] was 1 Hz at 1 s integration time and 0.7 Hz at 5 s integration time. The latter value is within a small factor of the estimate for the thermal noise. The chosen rotational period  $2\pi/\omega = 90$  s is a compromise—for shorter periods, the tilt control is not as accurate, for longer ones the number of rotations available for averaging is lower.

A number of systematic effects have been studied. We determined the sensitivities of the beat frequency to various external parameters. During data acquisition, we recorded tilts, transmitted laser wave powers, and environment temperature data simultaneously with the beat frequency. These parameters were analyzed in the same fashion as the beat frequency (see below), obtaining the corresponding modulation amplitudes. These amplitudes, together with the sensitivities, allow us to estimate the influence of the parameter variations on the amplitudes  $B$ ,  $C$ .

The sensitivity of the beat frequency to changes in power circulating in the two cavities was measured directly, (1.5, 5) Hz per 1% power variation, respectively. The means of the power modulation amplitudes at  $2\omega$  were less than  $1 \times 10^{-6}$  in relative units, implying a relative effect on the means of the coefficients  $B$ ,  $C$  of less than  $1 \times 10^{-18}$ .

The dependence of the beat frequency on rotational velocity (centrifugal effect) was measured by modulating the rotational speed. A velocity modulation with 10% relative amplitude caused a beat frequency modulation amplitude of 0.6 Hz. As the relative instability of the rotational velocity was only  $1 \times 10^{-6}$  on the time scale of 20 s, we do not expect any influence from this effect.

Sensitivities of the beat to tilts were determined at the beginning of each run. The values varied and were typically below 30 mHz/ $\mu$ rad for tilt in the vertical plane comprising the axis of cavity 1 and approximately 120 mHz/ $\mu$ rad for tilt in the orthogonal plane. The means of the amplitudes of the tilt modulations at  $2\omega$  were less than 0.2  $\mu$ rad, leading to an effect on the means of the coefficients  $B$ ,  $C$  of less than  $5 \times 10^{-17}$ .

From this analysis, only the tilt variations are considered important, and therefore the beat frequency data is corrected by subtracting the tilt values weighted with the appropriate sensitivities. The resulting data are used in the following analysis.

The beat frequency variation during each full rotation (labeled by  $i$ , centered at time  $t_i$ ) may be described by

$$\begin{aligned} [\nu_1(t) - \nu_2(t)]/\nu_0 = & \Delta(t_i) + a(t_i)t + A(t_i) + 2D(t_i)\sin\theta(t) \\ & + 2E(t_i)\cos\theta(t) + 2B(t_i)\sin 2\theta(t) \\ & + 2C(t_i)\cos 2\theta(t) + N_i(t), \end{aligned} \quad (1)$$

where  $\theta = \omega t$  is the angle of the cavity 1 with respect to the local south direction.  $A(t)$ ,  $B(t)$ ,  $C(t)$  are functions that describe isotropy violation according to specific test theories. Disturbing effects are described by the (slowly time-varying) coefficients  $a$  (drift due to temperature change or mechanical relaxation),  $D$ ,  $E$  (rotation-induced changes in

the apparatus' properties) and the short-term fluctuations  $N(t)$ .  $A(t)$  is modulated at the sidereal year period only and therefore cannot be experimentally distinguished from the long-term variations in  $a$  and  $\Delta$ , and is thus subsumed into the latter. A beat frequency drift quadratic in time is not explicitly included in Eq. (1). We extracted the slow frequency drift by smoothing the data with a running average function, determined the influence of this drift on the coefficients  $B$  and  $C$  and thereby obtained corrected values for them.

In common LLI violation models, the amplitudes  $B$ ,  $C$  are time-dependent functions because Earth's motion causes a varying orientation of the rotation axis (i.e., of the laboratory) with respect to an assumed preferred reference frame fixed to a certain celestial object. This will lead to a variation  $B(t)$ ,  $C(t)$  at the location of the experiment with the sidereal time  $t_\oplus$  corresponding to the laboratory time  $t$ . The SME applied to cavities [21] leads to the prediction  $C^p(t) = C_0(t_\oplus) + C_1(t_\oplus)\sin(\omega_\oplus t_\oplus) + C_2(t_\oplus)\cos(\omega_\oplus t_\oplus) + C_3(t_\oplus)\sin(2\omega_\oplus t_\oplus) + C_4(t_\oplus)\cos(2\omega_\oplus t_\oplus)$ , and a similar expression for  $B^p(t)$ . Each amplitude function  $C_n(t_\oplus)$  is a sum of a constant term and sine/cosine modulation terms at the orbital frequency  $\Omega_\oplus$ . The same is the case for the  $B_n(t_\oplus)$ , except for  $B_0$ , which is a constant. The amplitudes of the modulation terms are proportional to combinations of the three off-diagonal elements of the SME coupling coefficient matrix ( $\tilde{\kappa}_{o+}$ ), and are suppressed by a factor  $\beta_\oplus \simeq 1.0 \times 10^{-4}$  (ratio of earth orbital velocity and speed of light). The RMS test theory (with the effects of Earth's rotational velocity neglected) leads to expressions for  $B(t)$ ,  $C(t)$  with similar structure.

The data analyzed here were recorded during approximately 240 days spread over the interval of March 2008 to April 2009, and comprise approximately 175 000 rotations. The beat frequency recorded during each full rotation was least-squares fitted to expression (1), omitting the term  $N_i(t)$ . This produces a time series of amplitudes  $B(t_i)$ ,  $C(t_i)$ . Figure 2 shows the corresponding histograms. The standard deviations of the data of these two quantities are  $(7.5, 6.1) \times 10^{-16}$ , respectively. These values indicate the single-rotation sensitivity level for an anisotropy signal. The mean of the amplitudes  $B(t_i)$  exhibits a larger deviation from zero ( $1.2 \times 10^{-17}$ ) than that of  $C(t_i)$ . Figure 3 shows the data with the time axis folded back on itself with the period of one sidereal day and then averaged, so as to simplify the display.

We search for a LLI violation by fitting the RMS and SME models' predicted time variations to the time series  $B(t_i)$ ,  $C(t_i)$ . In order to partially account for unidentified systematic effects that may vary from run to run, we first fit the time series of each of the  $M = 46$  data runs exceeding 1 d in length and having low perturbations (totalling approximately 135 000 rotations) to expressions  $B^p(t)$ ,  $C^p(t)$  as given above with amplitudes  $(B_0, \dots, C_4)_k$  assumed constant over the duration of each data run  $k$ . Subsequently, the RMS and SME models are fitted to the  $M$  amplitude sets, disregarding the  $B_0$  values.

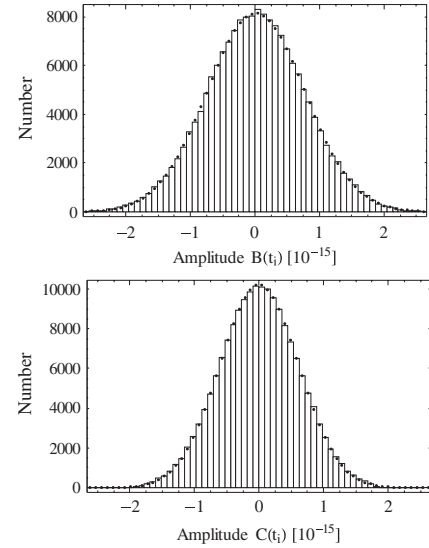


FIG. 2. Histograms of the measured modulation amplitudes (all data). For comparison, the dots indicate the histogram values of a Gaussian distribution with the same mean and variance as the corresponding data set.

In the RMS model, conventionally, the assumed preferred frame is at rest with respect to the cosmic microwave background radiation field. Nonzero values of three dimensionless parameters,  $\alpha + 1/2$ ,  $\delta$ , and  $\beta - 1/2$  describe modifications of the usual Lorentz transformations. The

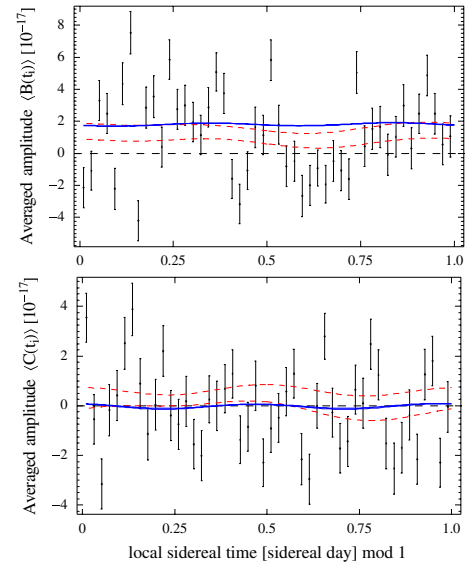


FIG. 3 (color online). Isotropy violation signals. Points: mean values of the modulation amplitudes measured within 0.5 h intervals during each sidereal day (all data). The error bars indicate the statistical standard errors of the means. Full lines (blue): range of values that the RMS violation signals (not averaged) for the fitted value  $\delta - \beta + \frac{1}{2}$  of Eq. (2) and a systematic offset on  $B$  take on during 1 yr. The two full lines lie very close since Earth's orbital velocity is small compared to the solar system velocity. Dashed lines (red): same for the SME violation signals (not averaged) given by the fitted values of Eq. (3).

combination  $\delta - \beta + 1/2$  also quantifies the directional dependence of the speed of light in a frame moving with velocity  $v$  with respect to the preferred frame,  $\Delta c(\psi)/c_0 = (\delta - \beta + \frac{1}{2})(v/c_0)^2 \sin^2 \psi$ .  $\psi$  is the angle between the light propagation direction and the laboratory velocity vector. For a laboratory on Earth, the time-averaged value of  $v$  is the solar system velocity,  $\approx 3.7 \times 10^5$  m/s. Applying this expression to a rotating cavity pair predicts a particular time dependence of the beat frequency, in which  $B^p(t)$  and  $C^p(t)$  are proportional to  $\delta - \beta + \frac{1}{2}$ . We find

$$\delta - \beta + \frac{1}{2} = (-1.6 \pm 6 \pm 1.2) \times 10^{-12}. \quad (2)$$

The first error is the statistical  $1\sigma$  error, the second is the estimated systematic error due to the uncertainty in the determination of the tilt sensitivities. The corresponding RMS amplitude functions are shown in Fig. 3 as full lines.

The SME model fit yields

$$\begin{aligned} (\tilde{\kappa}_{e-})^{ZZ} &= (1.6 \pm 2.4 \pm 1.1) \times 10^{-17}, \\ (\tilde{\kappa}_{e-})^{XY} &= (0.0 \pm 1.0 \pm 0.3) \times 10^{-17}, \\ (\tilde{\kappa}_{e-})^{YZ} &= (-0.6 \pm 1.4 \pm 0.5) \times 10^{-17}, \\ (\tilde{\kappa}_{e-})^{XZ} &= (0.4 \pm 1.5 \pm 0.1) \times 10^{-17}, \\ (\tilde{\kappa}_{e-})^{XX} - (\tilde{\kappa}_{e-})^{YY} &= (0.8 \pm 2.0 \pm 0.3) \times 10^{-17}, \\ (\tilde{\kappa}_{o+})^{XY} &= (1.5 \pm 1.5 \pm 0.2) \times 10^{-13}, \\ (\tilde{\kappa}_{o+})^{YZ} &= (-0.1 \pm 1.0 \pm 0.4) \times 10^{-13}, \\ (\tilde{\kappa}_{o+})^{XZ} &= (-0.1 \pm 1.0 \pm 0.2) \times 10^{-13}. \end{aligned} \quad (3)$$

The errors given are found as for the RMS fit. The coefficient  $(\tilde{\kappa}_{e-})^{ZZ}$  is predominantly determined by the long-time-average value of  $C_0$ . While the latter is quite small ( $2.2 \times 10^{-18}$ ), the average value of  $B_0$  is relatively large,  $\langle(B_0)_k\rangle \cong 1.8 \times 10^{-17}$ , which nevertheless has little influence on the fitted values in Eq. (3). From an experimental point of view, both  $\langle(B_0)_k\rangle$  and  $\langle(C_0)_k\rangle$  could be sensitive to systematic effects to a similar extent. We cannot rule out that a systematic effect on  $\langle(C_0)_k\rangle$  of value comparable to  $\langle(B_0)_k\rangle$  (which is comparable to the sample standard deviations of both  $(B_0)_k$  and  $(C_0)_k$ ) could cancel a LLI violation arising from a corresponding nonzero  $(\tilde{\kappa}_{e-})^{ZZ} \sim 1.2 \times 10^{-16}$ . Therefore, we conservatively take this as an additional systematic error of that coefficient.

All mean values fall within their  $1\sigma$  total uncertainties. Figure 3 reports as dashed lines the value ranges that the best-fit SME amplitude functions  $B^p(t_\oplus)$ ,  $C^p(t_\oplus)$  take during 1 yr.

In conclusion, we find no clear evidence for a violation of isotropy of the frequency of a linear electromagnetic cavity, analyzed either within the RMS model, or within the SME limited to the photonic sector. The  $1\sigma$  uncertainties of the SME violation coefficients  $(\tilde{\kappa}_{e-})$  and  $\beta_\oplus(\tilde{\kappa}_{o+})$  are equal to or less than  $2 \times 10^{-17}$ , except for  $(\tilde{\kappa}_{e-})^{ZZ}$ , where a conservative estimate is  $12 \times 10^{-17}$ . Within the RMS model our experiment shows that the anisotropy of

the speed of light on Earth,  $(1/2)|\Delta c(\pi/2)|/c_0$ , is less than  $0.6 \times 10^{-17}$  ( $1\sigma$  level). These results represent a strong improvement on previous experiments. We stress that, independent of the particular model used in deriving violation coefficients (and the interpretation in terms of isotropy of  $c$  given here), the experimental results represent a strong test of one aspect of local Lorentz invariance, the independence of the outcome of experiments from orientation.

Ch. E. is grateful to the Gründerstiftung Düsseldorf for financial support. We thank M. Okhapkin for his contributions to the development of the apparatus, and P. Dutkiewicz and R. Gusek. This work has been funded by the DFG.

- 
- [1] A. Brillet and J. L. Hall, Phys. Rev. Lett. **42**, 549 (1979); for overviews, see, e.g., D. Mattingly, Living Rev. Relativity **8**, 5 (2005); V. A. Kostelecky and N. Russell, arXiv:0801.0287; *Special Relativity*, edited by J. Ehlers and C. Lämmerzahl, Lecture Notes in Physics (Springer, New York, 2006), Vol. 702; *CPT and Lorentz Symmetry IV*, edited by V. A. Kostelecky (World Scientific, Singapore, 2008), and references therein.
  - [2] J. A. Lipa, J. A. Nissen, S. Wang, D. A. Stricker, and D. Avaloff, Phys. Rev. Lett. **90**, 060403 (2003).
  - [3] H. Müller, S. Hermann, C. Braxmaier, S. Schiller, and A. Peters, Phys. Rev. Lett. **91**, 020401 (2003).
  - [4] S. Schiller, P. Antonini, and M. Okhapkin, in *Lecture Notes in Physics* (Springer, New York, 2006), Vol. 702, pp. 401–415.
  - [5] S. Hermann, A. Senger, E. Kovalchuk, H. Müller, and A. Peters, Phys. Rev. Lett. **95**, 150401 (2005).
  - [6] P. L. Stanwix *et al.*, Phys. Rev. Lett. **95**, 040404 (2005); Phys. Rev. D **74**, 081101(R) (2006).
  - [7] R. K. Mittleman, I. I. Ioannou, H. G. Dehmelt, and N. Russell, Phys. Rev. Lett. **83**, 2116 (1999).
  - [8] G. W. Bennett *et al.*, Phys. Rev. Lett. **100**, 091602 (2008).
  - [9] F. Cane *et al.*, Phys. Rev. Lett. **93**, 230801 (2004).
  - [10] P. Wolf *et al.*, Phys. Rev. D **70**, 051902(R) (2004).
  - [11] P. Wolf, F. Chapelet, S. Bize, and A. Clairon, Phys. Rev. Lett. **96**, 060801 (2006).
  - [12] H. Müller *et al.*, Phys. Rev. Lett. **99**, 050401 (2007).
  - [13] V. A. Kostelecky and M. Mewes, Phys. Rev. Lett. **97**, 140401 (2006).
  - [14] F. R. Klinkhamer and M. Risse, Phys. Rev. D **77**, 016002 (2008); with additional information in arXiv:0709.2502v5.
  - [15] S. Reinhardt *et al.*, Nature Phys. **3**, 861 (2007).
  - [16] P. Wolf *et al.*, Phys. Rev. Lett. **90**, 060402 (2003).
  - [17] A. A. Michelson and E. W. Morley, Am. J. Sci. **34**, 333 (1887).
  - [18] H. P. Robertson, Rev. Mod. Phys. **21**, 378 (1949).
  - [19] R. Mansouri and R. U. Sexl, Gen. Relativ. Gravit. **8**, 809 (1977).
  - [20] D. Colladay and V. A. Kostelecký, Phys. Rev. D **55**, 6760 (1997).
  - [21] V. A. Kostelecký and M. Mewes, Phys. Rev. D **66**, 056005 (2002).
  - [22] Ch. Eisele, M. Okhapkin, A. Y. Nevsky, and S. Schiller, Opt. Commun. **281**, 1189 (2008).